© 2025 Journal of Pharmacy & Pharmacognosy Research, 13 (4), 1275-1287, 2025
ISSN 0719-4250
https://jppres.com

DOI: https://doi.org/10.56499/jppres24.2178_13.4.1275

Original Article

A xanthone from *Garcinia lateriflora* Blume leaves extract: Isolation, α-glucosidase inhibitory activity, and antioxidant capacity

[Xantona del extracto de hojas de *Garcinia lateriflora*: Aislamiento, actividad inhibidora de la α-glucosidasa y capacidad antioxidante]

Putu G.M.W. Mahayasih[1*], Muhammad Hanafi[2], Yonatan Eden[1], Dimas Maulana[1], Nita Triadisti[3], Berna Elya[4*]

[1]Department of Pharmacy, Faculty of Health and Sciences, Universitas Esa Unggul, Jakarta, 11530, Indonesia.
[2]Research Centre for Pharmaceutical Ingredients and Traditional Medicine, National Research and Innovation Agency (BRIN), Serpong, 15314, Indonesia.
[3]Faculty of Pharmacy, Universitas Muhammadiyah Banjarmasin, Banjarmasin, 70115, Indonesia.
[4]Department of Pharmacognosy and Phytochemistry, Faculty of Pharmacy, Universitas Indonesia, Depok, 16424, Indonesia.
[*]E-mail: putu.gitamaya@esaunggul.ac.id; berna.elya@farmasi.ui.ac.id

Abstract

Context: The leaf extracts of *Garcinia lateriflora* have activity as α-glucosidase inhibitor and antioxidant. α-glucosidase inhibitor is one of the mechanisms that can treat type 2 diabetic mellitus (T2DM).

Aims: To isolate and identify the molecule responsible for the antioxidant activities and α-glucosidase enzyme inhibition of *G. lateriflora* leaf extract.

Methods: The leaves of *G. lateriflora* were progressively extracted using the maceration method with n-hexane (He), ethyl acetate (EA), and methanol (Me). The isolation procedure used column chromatography, employing the stationary phase of silica gel 60 and Sephadex LH20. The *in vitro* activity of alpha-glucosidase inhibition was examined using p-nitrophenyl-α-D-glucopyranoside as the substrate. The antioxidant activity was assessed using the DPPH radical scavenging and FRAP assay.

Results: Fraction EA12 has greater efficacy in inhibiting the α-glucosidase enzyme and acts as a more potent antioxidant. Compounded EA12a was obtained by further purification and isolation at Fraction EA12. The IC_{50} value for inhibiting α-glucosidase was determined to be 3.63 ± 0.01 µg/mL. The antioxidant activity, as measured by the FRAP assay, had an IC_{50} value of 27.08 ± 0.26 µg/mL, while the DPPH radical scavenging assay yielded an IC_{50} value of 21.31 ± 0.22 µg/mL. The compound EA12a was structurally elucidated using 1H-NMR and LC-MS/MS, revealing its probable structure as 1,3,6,7-tetrahydroxyxanthone.

Conclusions: In this study, 1,3,6,7-tetrahydroxyxanthone was identified in *G. lateriflora* leaves extract with α-glucosidase inhibitory and antioxidant activity.

Keywords: *Garcinia*; hyperglycemia; plant; prediabetic; 1,3,6,7-tetrahydroxyxanthone.

Resumen

Contexto: Los extractos de hojas de *Garcinia lateriflora* tienen actividad como inhibidor de la α-glucosidasa y antioxidante. La inhibición de la α-glucosidasa es uno de los mecanismos que pueden tratar la diabetes mellitus tipo 2 (T2DM).

Objetivos: Aislar e identificar la molécula responsable de las actividades antioxidantes y la inhibición de la enzima α-glucosidasa del extracto de hojas de *G. lateriflora*.

Métodos: Las hojas de *G. lateriflora* se extrajeron progresivamente utilizando el método de maceración con n-hexano (He), acetato de etilo (EA) y metanol (Me). El procedimiento de aislamiento utilizó cromatografía en columna, empleando la fase estacionaria de gel de sílice 60 y Sephadex LH20. La actividad in vitro de inhibición de la α-glucosidasa se examinó utilizando p-nitrofenil-α-D-glucopiranósido como sustrato. La actividad antioxidante se evaluó utilizando el análisis de radicales DPPH y el ensayo FRAP.

Resultados: La fracción EA12 tiene una mayor eficacia en la inhibición de la enzima α-glucosidasa y actúa como un antioxidante más potente. El compuesto EA12a se obtuvo mediante una purificación y aislamiento adicionales en la fracción EA12. El valor de IC_{50} para la inhibición de la α-glucosidasa se determinó en 3,63 ± 0.01 µg/mL. La actividad antioxidante, medida mediante el ensayo FRAP, tuvo un valor de IC_{50} de 27,08 ± 0.26 µg/mL, mientras que el ensayo de eliminación de radicales DPPH arrojó un valor de IC_{50} de 21,31 ± 0.22 µg/mL. El químico EA12a se dilucidó estructuralmente utilizando 1H-NMR y LC-MS/MS, revelando su probable estructura como 1,3,6,7-tetrahidroxixantona.

Conclusiones: El compuesto 1,3,6,7-tetrahidroxixantona fue identificado en el extracto de hojas de *G. lateriflora* con actividad antioxidante e inhibidora de la α-glucosidasa.

Palabras Clave: *Garcinia*; hiperglucemia; planta; prediabético; 1,3,6,7-tetrahidroxixantona.

ARTICLE INFO
Received: August 15, 2024.
Accepted: March 14, 2025.
Available Online: May 6, 2025.

AUTHOR INFO
ORCID: 0000-0002-7434-4493 (PGMWM) 0000-0001-6123-2356 (NT)
0000-0003-4127-5281 (MH) 0000-0003-2904-6515 (BE)
0000-0001-7140-1432 (YE)

INTRODUCTION

Type 2 diabetes mellitus (T2DM) is one of the major metabolic disorders characterized by hyperglycemia and impaired insulin action or secretion. The prevalence of T2DM has rapidly increased in the past decade, and without any interventional approaches, global cases of T2DM will increase to more than 350 million by 2030 (Ogurtsova et al., 2017). Insulin resistance due to disrupted insulin signaling pathways is considered to play a central role in the development of chronic hyperglycemia. One of the early hallmarks of T2DM, postprandial hyperglycemia, activates oxidative stress through the over-formation of free radicals, which can be associated with various complications, such as cardiovascular disease. As a result, attenuation of postprandial hyperglycemia by delaying glucose absorption has become a key therapeutic target for diabetes management (Akmal et al., 2024). Therefore, efforts have been directed toward inhibiting α-glucosidase, a major enzyme for carbohydrate digestion in the small intestine. Some existing α-glucosidase inhibitors, such as acarbose and voglibose, are already clinically available and elicit gastrointestinal adverse effects (Dirir et al., 2022).

Exploration and continuous testing of secondary metabolite compounds from different plant sources are still needed to find alternative medicine for T2DM from natural compounds, especially on the mechanism of inhibiting the α-glucosidase enzyme. Around 30,000 different species of medicinal plants exist around Indonesia, of which 25% have herbal properties (Mottaghipisheh et al., 2024). *Garcinia* is a genus of plants from the family *Clusiaceae*, with more than 418 species, 64 of which are found in some areas in Indonesia. Among the mentioned species are *Garcinia mangostana*, *G. cambogia,* and *G. brasiliensis,* among others, which are highly used in health applications for various reasons, including relief from stomach pain, curing of chronic ulcers, healing of infected wounds, diarrhea control, treatment of cancer, heart diseases, and also the various degenerative diseases (El-Lateef et al., 2023; Espirito Santo et al., 2020).

Most of the varied advantages and activities of the *Garcinia* plant chemicals are due to secondary metabolites. Secondary metabolites of the *Garcinia* plant include flavonoids, tannins, and xanthones, mainly found in fruit peels and leaves. Xanthone is a polyphenol displaying an unusual, attractive structure of three cyclic aromatic rings in a C6-C3-C6 pattern (Amelia et al., 2015; Huang et al., 2021). Xanthone found in the genus *Garcinia*, such as mangosteen, has been reported as an antiviral, anti-inflammatory, antitumoral, antibacterial, antidiabetic, and antioxidant (El-Lateef et al., 2023; Espirito Santo et al., 2020), so it still has potential for studying other xanthone compounds from the genus *Garcinia*.

One of the species belonging to the genus *Garcinia* is *Garcinia lateriflora* Blume, which flourishes in regions characterized by elevated humidity and relatively brief summer seasons, such as Indonesia. This plant thrives at 1000 meters (20-40°C) in tropical regions and experiences ideal growth in low-lying areas. From the previous study, the ethyl acetate extract from *G. lateriflora* leaves posed very strong activity as α-glucosidase inhibitors and antioxidants compared with n-hexane and methanol extracts. Further fractionation process using column chromatography on the ethyl acetate extract resulted in some fractions with better α-glucosidase inhibitor and antioxidant activity on scavenging radical 1,1-diphenyl-2-picrylhydrazyl (DPPH) and reducing ferric reducing antioxidant power (FRAP) reagent than the extract (Mahayasih et al., 2017; 2018). But to the best of our knowledge, there is no study on exploring and isolating the active compound from *G. lateriflora* as an α-glucosidase inhibitor and with antioxidant activity. Therefore, this research aimed to isolate secondary metabolite compounds from the leaves of *G. lateriflora.* The compound 1,3,6,7-tetrahydroxyxanthone was successfully isolated from the leaves of *G. lateriflora.* Afterward, a test was conducted to measure the inhibitory activity of the α-glucosidase enzyme *in silico* and *in vitro,* and its enzyme kinetics and antioxidant activity of the isolated compound 1,3,6,7-tetrahydroxyxanthone.

MATERIAL AND METHODS

Plant material

Garcinia lateriflora leaves were collected from Bogor Botanical Garden, Indonesia (6°35'53"S 106°47'57"E) and were identified by The Centre for Plant Conservation from Bogor Botanical Garden with a registered number of B-1990/IPH.4/KS/XI/2019.

Extraction and isolation

Five kilograms of dried leaves of *G. lateriflora* were macerated sequentially with distillate n-hexane, ethyl acetate, and methanol at room temperature for 24 hours. Extracts were evaporated using a rotary evaporator (Buchi rotavapor TMR-100, Canada) to obtain the n-hexane, ethyl acetate, and methanol crude extract. Each step of maceration was repeated three times.

Twenty-five grams of ethyl acetate extracts of *G. lateriflora* were fractionated by loaded-to-column

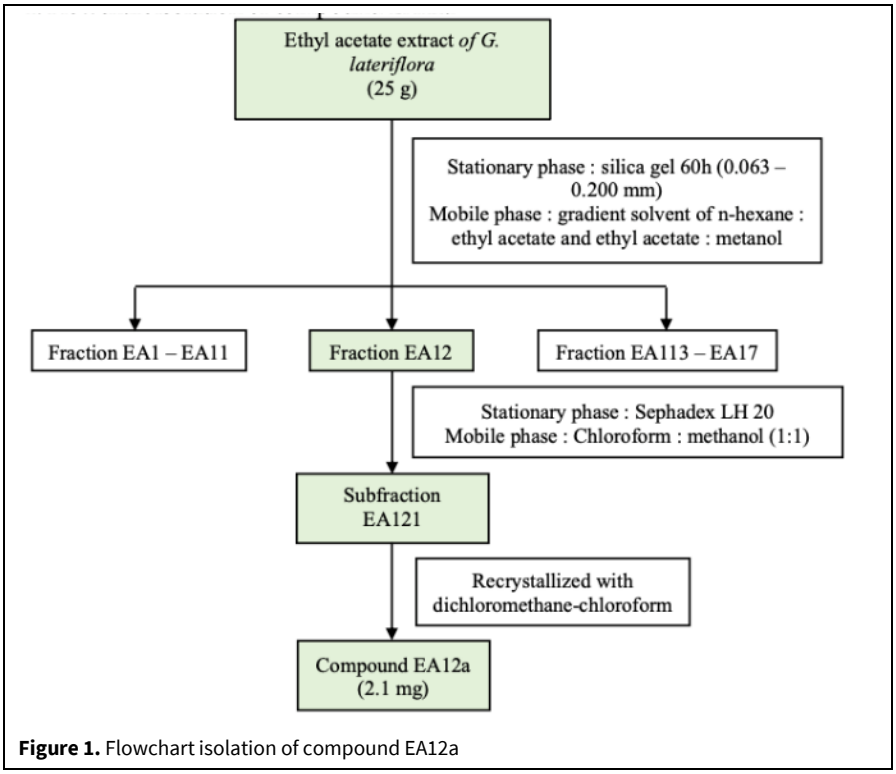


Figure 1. Flowchart isolation of compound EA12a

chromatography with silica gel 60 (Merck, 0.063–0.200 mm) as stationary phase and eluted successively with a combination mobile phase of distillate n-hexane – n-hexane:ethyl acetate – ethyl acetate – ethyl acetate:methanol and methanol in a gradient polarity solvent. This process was afforded 17 fractions based on its thin-layer chromatography profile using a TLC plate (silica gel GF254 aluminium sheets, Merck) and viewer with UV lamp 254 nm and 366 nm (CAMAG® UV Cabinet 4) (Mahayasih et al., 2017; 2018).

A quantity of 635 mg of fraction 12 (EA12) was then re-chromatographed on Sephadex LH 20 as the stationary phase and eluted with isocratic solvents chloroform:methanol (1:1). The subfraction, which had the same thin layer chromatography pattern, was combined and obtained subfraction EA121. It was recrystallized with dichloromethane-chloroform to afford a yellow-brown powder of compound EA12a (2.1 mg). The compound was elucidated with LC-MS/MS (Waters, USA) and ^{1}HNMR (Jeol, Japan) spectroscopies (Delita et al., 2020). The flowchart of the isolation of compound EA12a can be shown in Fig. 1.

α-glucosidase inhibitory activity

The α-glucosidase inhibitory activity was conducted based on the methods described by Mahayasih et al. (2017). The testing was conducted *in vitro* with p-nitrophenyl-α-D-glucopyranoside (p-NPG) as the substrate (Sigma-Aldrich, USA). Thirty microliter samples in serial concentration were put with 17 µL of 4 mM substrate p-NPG and 36 µL of phosphate buffer (Merck, USA), pH 6.8, in 96-well microplates (Scientific Consumables and Instrumentation, USA). The mixture was incubated at 37°C for 5 minutes. Add 17 µL of the 0.8 unit/L α-glucosidase enzyme (Sigma-Aldrich, USA) into the mixture and further incubate for another 15 minutes until the reaction is complete. Add 100 µL of the 267 mM Na_2CO_3 solution (Sigma-Aldrich, USA) to stop the reaction. Read the absorbance of the mixture using a microplate reader (Versamax ELISA Microplate Reader, USA) at 400 nm. The same test was conducted three times with acarbose (Sigma-Aldrich, USA) as the standard. The inhibition (%) was determined by equation [1].

$$\text{Inhibition (\%)} \quad \frac{\text{Abs blank} - \text{Abs sample}}{\text{Abs blank}} \times 100 \qquad [1]$$

Where, absorption (Abs) of blank was considered the absorbance of a solution that only has the enzyme and the substrate pNPG. A solution that only had a substrate pNPG and the tested sample served as a control sample. GraphPad Prism 7.0 software was used to calculate the IC_{50} value.

α-glucosidase enzyme inhibitory kinetics

Inhibition kinetics were assessed following the methodology outlined by Rouzbehan et al. (2017). Briefly, a fixed concentration of α-glucosidase was incubated with increasing concentrations of its substrate, p-NPG, at 37°C for 15 min. This incubation occurred in both the absence and presence of the test samples, with the sample concentration equivalent to

their half-maximal inhibitory concentration (IC_{50}). Following incubation, reactions were terminated, and the absorbance was measured. The absorbance data were then converted to reaction rates using the Lineweaver-Burk plot. All determinations were performed in triplicate.

In silico investigation of α-glucosidase-inhibitor interaction

This study employed AutoDock Vina (v1.5.7) to computationally simulate the interaction mechanism between α-glucosidase and inhibitor molecules, specifically compound EA12a (Nur et al., 2023; Shen et al., 2022). This approach facilitates the prediction of potential binding affinities between inhibitors and the enzyme. The α-glucosidase crystal structure (PDB ID: 5NN8) was retrieved from the Protein Data Bank (https://www.rcsb.org/). The structures of compound EA12a were generated using ChemDraw Pro 12.0 software. For the docking simulation, the center coordinates of the binding box for the α-glucosidase (PDB ID: 5NN8) were defined as (-13.373, -38.238, -95.028). The lattice points in each direction of the XYZ axes were fixed at 12 × 21 × 11. The protein structure was treated as rigid during the simulation. The binding energies of ligands bound to the active sites were analyzed using AutoDock Tools to identify the conformation with the most favorable score.

ADMET prediction

The basic physicochemical properties, pharmacokinetic characteristics, and drug-likeness were predicted using SwissADME (http://www.swissadme.ch/) online tools. Meanwhile, the toxicity was predicted using ProTox 3.0 (https://tox.charite.de/) online tools (Subhan et al., 2025). The canonical simplified molecular input line entry (SMILE) representations of acarbose were obtained from the PubChem server (https://pubchem.ncbi.nlm.nih.gov/), while the compound EA12a structure was drawn using Marvin JS and converted into a canonical SMILES using SwissADME. The canonical SMILES of acarbose and compound EA12a were submitted to each software application, and Microsoft Excel was used to compile and process the data.

Antioxidant capacity

The antioxidant capacity of *G. lateriflora* leaf was investigated using two antioxidant assay methods: the DPPH assay and the FRAP assay. The procedure followed the previous method described by Mahayasih et al. (2018), and quercetin was used as the positive control.

DPPH assay

DPPH assay was performed using a 96-well microplate reader (Versamax ELISA Microplate Reader, USA). All the sample and standard quercetin (Sigma-Aldrich, USA) were dissolved in methanol to obtain several concentration levels. Twenty microliters of sample solution in methanol with serial concentrations were placed on a 96-well microplate (Scientific Consumables and Instrumentation, USA), and 180 µL of 150 mM DPPH solution (Sigma-Aldrich, USA) were added. The mixture was shaken up for 30 min at room temperature in the dark conditions, and the absorbance of the mixture was measured at a wavelength of 517 nm. The sample's ability to scavenge DPPH radical was calculated by equation [2]. The EC_{50} was analyzed using GraphPad Prism 7.0 software (GraphPad Software, USA).

$$\text{DPPH scavenged (\%)} \quad \frac{\text{Abs control} - \text{Abs sample}}{\text{Abs control}} \times 100 \qquad [2]$$

Where, Abs sample is the absorbance of sample, and Abs control the absorbance of solvent (methanol). The starting absorbance of DPPH (absorbance of control) was between 0.650 and 0.750.

FRAP assay

Thirty microliters of standard and sample solution in methanol were put in a 96-microplate well, and 270 µL of FRAP reagent (Sigma-Aldrich, USA) were added to the sample solution. The FRAP reagent was prepared by mixing 10 mL of 10 mM TPTZ solution (Sigma-Aldrich, USA) in 40 mM HCl with 100 mL of acetate buffer pH 3.6 and 10 mL of 20 mM $FeCl_3.6H_2O$ solution (Sigma-Aldrich, USA). The mixture must be incubated for 30 min to complete the reaction. The Versamax ELISA microplate reader (VersaMax, USA) was used to record the absorbance of the sample and standard at 593 nm. The percent inhibition (I%) was calculated by equation [3]. EC_{50} value was calculated using the GraphPad Prism 7.0 software.

$$\text{I (\%)} = (\text{Abs sample} - \text{Abs blank}) \times 100\% \qquad [3]$$

Where, Abs sample is the sample absorbance at 593 nm, and Abs blank the solvent (methanol) absorbance at 593 nm. The starting absorbance of FRAP (blank absorbance) was between 0.07 and 0.09.

Statistical analysis

The mean and the standard deviation were calculated using Microsoft Excel, and the data were presented as mean ± SD. The IC_{50} value of the α-glucosidase inhibitor and EC_{50} value of the antioxidant assay were calculated using GraphPad Prism 7.0 software (GraphPad Software, USA). The significant differences in mean from each group (n = 3) were calculated by the SPSS 25 version (IBM Corp., Armonk, USA), combining ANOVA and Tukey's test ($p<0.05$). The data correlation between antioxidant

capacity (FRAP and DPPH method) and α-glucosidase inhibitory activity of extract, fraction, and compound EA12a was examined by Pearson correlation analysis using SPSS 25.

RESULTS AND DISCUSSION

Spectral data of compound EA12a

In this study, we obtained 2.1 mg of yellow-brown powders named compound EA12a. The LC-MS/MS data in Fig. 2 shows that the peak was at m/z 261.07 [M+]. The ^{1}H-NMR spectrum data (acetone-d6, 500 MHz) in Fig. 3 indicated the presence of several signal groups consisting of six protons. A singlet signal at δH 13.23 (^{1}H, *s*) indicates the presence of a hydroxyl group in the aromatic ring that forms a chelate with another carbonyl group. The aromatic proton can be shown by two para-coupled signals at δH 6.91 and 7.52 (each ^{1}H, *s*) and two *meta*-coupled signals at δH = 6.21 and 6.37 (each ^{1}H, *d*, *J* = 1.9 Hz). A singlet signal at δH 8.02 probably indicated the presence of two protons on hydroxyl groups that were placed symmetrically with each other.

Based on spectroscopic data and supported by previous literature (Amelia et al., 2015) and prediction of the ^{1}H-NMR spectrum with ChemDraw Software, the EA12a compound is assumed to be 1,3,6,7-tetrahydroxyxanthone with a molecular formula of $C_{13}H_8O_6$. The structure of the compound can be seen in Fig. 4, and the comparison of ^{1}H-NMR chemical shift data between the EA12a compound and data in previous studies by Amelia et al. (2015) can be seen in Table 1.

The discovery of compound 1,3,6,7-tetrahydroxyxanthone in *G. lateriflora* was not surprising, as it has been found before in the genus *Garcinia*, especially from the species *G. brasiliensis* epicarp and *G. mangostana* (Gontijo et al., 2012).

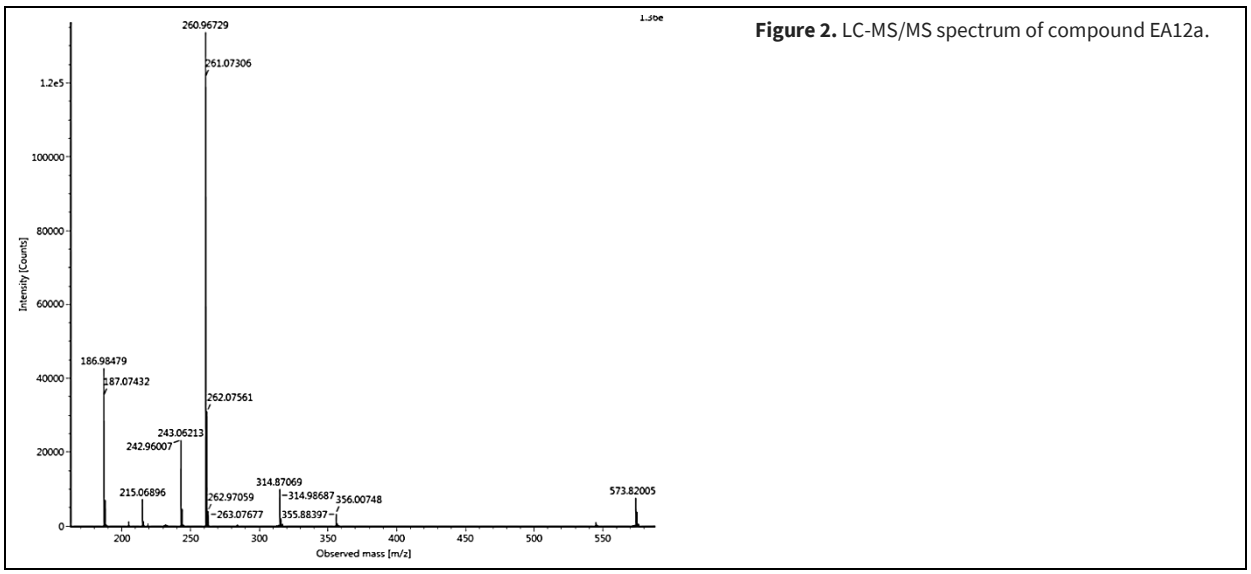


Figure 2. LC-MS/MS spectrum of compound EA12a.

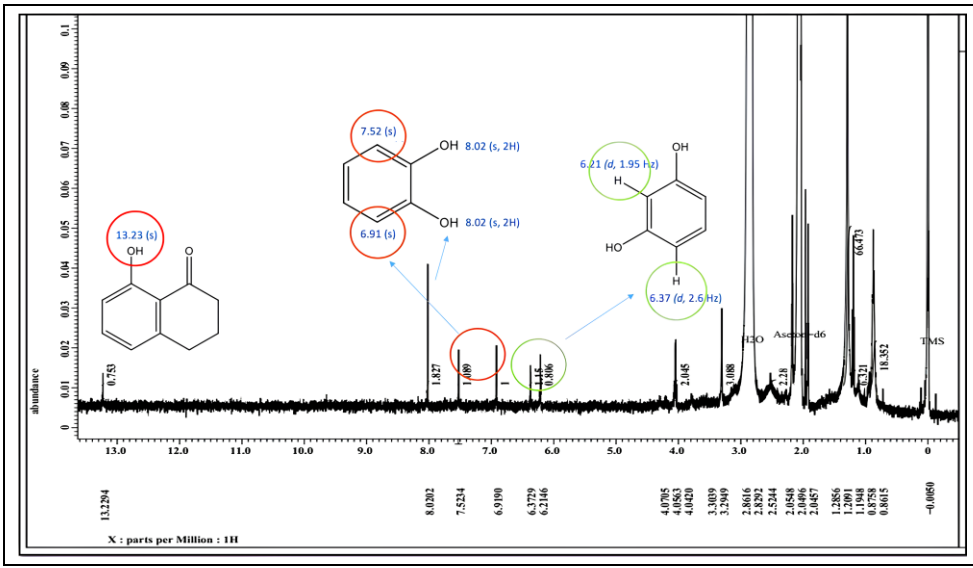


Figure 3. ^{1}H-NMR Spectrum of compound EA12a (CD_3OD, 500 MHz).

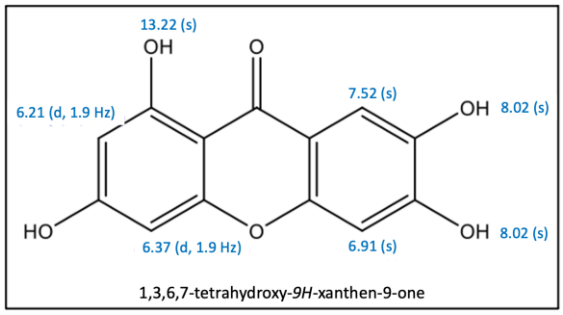


Figure 4. The predicted structure of compound EA12a.

Table 1. Comparison of the chemical shift of the ^{1}H-NMR spectrum between compound EA12a with 1,3,6,7-tetrahydroxyxanthone (CD_3OD, 500 MHz).

Atom H	1,3,6,7-tetrahydroxyxanthone δH (ppm)	EA12a δH (ppm)
1-OH	13.85 (s)	13.02 (s)
H-2	6.15 (*d, J*= 2 Hz)	6.21 (*d, J*= 1,9 Hz)
H-4	6.29 (*d, J*= 2 Hz)	6.37 (*d, J*= 1,9 Hz)
H-5	6.83 (s)	6.91 (s)
H-8	7.44 (s)	7.52 (s)
6-OH	-	8.02 (s)
7-OH	-	8.02 (s)

Table 2. The α-glucosidase inhibitory and antioxidant capacity of ethyl acetate extract, fraction EA12, and compound EA12a.

Sample	IC_{50} (µg/mL)	EC_{50} (µg/mL)	
	α-glucosidase inhibitor	DPPH assay	FRAP assay
Ethyl acetate extract (EAE)	34.79 ± 0.12*	65.20 ± 0.45*	48.61 ± 0.32*
Fraction EA12	17.90 ± 0.11*	102.08 ± 0.75*	>79.5
Compound EA12a	3.63 ± 0.01*	21.31 ± 0.22*	27.08 ± 0.26*
Acarbose	39.53 ± 0.24*	Nt	Nt
Quercetin	Nt	3.96 ± 0.02*	10.74 ± 0.32*

Data are expressed as mean ± SD (n = 3). *Means values in a column are statistically significant ($p<0.05$). Nt: Not tested.

α-glucosidase activity of compound EA12a

Compound EA12a is a compound obtained from purifying the ethyl acetate extract fraction of *G. lateriflora* number 12 (EA12). In the previous study, it was known that the ethyl acetate extract of *G. lateriflora* leaf has better activity in inhibiting the α-glucosidase enzyme than acarbose (IC_{50} 39.53 ± 0.24 µg/mL), with an IC_{50} value of 34.79 ± 0.12 µg/mL (Mahayasih et al., 2017). This study also investigated the α-glucosidase inhibitory activity of EA12 fraction and compound EA12a. The result can be seen in Table 2.

A test for α-glucosidase was conducted using p-NPG as the substrate. The α-glucosidase enzyme will hydrolyze p-NPG, and the inhibitory activity of α-glucosidase is indicated by changes in the intensity of the color of p-nitrophenol from yellow to clear. The data from Table 2 showed that compound EA12a has the highest activity in inhibiting the α-glucosidase enzyme compared to its extract, fraction, and acarbose as a positive control, with the IC_{50} value of compound EA12a being 3.63 ± 0.01 µg/mL ($p<0.05$). Based on Fig. 5, the α-glucosidase inhibitory activity of ethyl acetate extract, fraction EA12, compound EA12a, and acarbose in inhibiting α-glucosidase enzyme showed a dose-dependent manner. The ability of the sample to inhibit the α-glucosidase enzyme will increase as the dose increases. Thus, the compound EA12a had the potency to develop as an α-glucosidase inhibitor.

The a-glucosidase enzyme inhibitory kinetics

To elucidate the specific mode of inhibition—competitive, noncompetitive, uncompetitive, or

mixed—researchers commonly employ techniques that transform nonlinear kinetic data into linear relationships (Rouzbehan et al., 2017). The Lineweaver-Burk plot is a widely used method for this purpose. The α-glucosidase kinetic analysis of compound EA12a (1,3,6,7-tetrahydroxyxanthone) is presented in Fig. 6.

Analysis of the Lineweaver-Burk plot revealed that both inhibitory mechanisms of 1,3,6,7-tetrahydroxyxanthone are mixed-type. Both these inhibitors bind with the free enzyme and the enzyme-substrate complex, altering the apparent affinity between the enzyme and the substrate. The Km observed increases or decreases depending on whether the inhibitor binds preferentially to the free enzyme or the enzyme-substrate complex. The fact that the extracts can bind to other sites on the enzyme apart from the active site means they can potentially have a broader inhibition spectrum than acarbose, a competitive inhibitor (Shen et al., 2022).

One major advantage of these mixed inhibitors compared to acarbose is that they may still be effective at higher substrate concentrations. Because acarbose is a competitive inhibitor, its inhibition is weakened at high substrate levels, whereas the mixed inhibitor would reduce enzyme activity under conditions of increased substrate availability (Rouzbehan et al., 2017; Shen et al., 2022).

In silico investigation of compound EA12a

Molecular docking technology is a tool for analyzing the interaction between macromolecular receptors and small-molecule ligands. It can accurately identify the potential binding sites for ligands and determine their spatial conformations (Elwekeel et al., 2022). The current work utilized a molecular docking simulation technique to study the binding locations of compound EA12a, 1,3,6,7-tetrahydroxyxanthone, to α-glucosidase. In contrast to the *in vitro* study, 1,3,6,7-tetrahydroxyxanthone exhibits a lower binding energy in molecular docking simulations. The α-glucosidase enzyme exhibited an optimal binding energy of -7.087 kcal/mol with 1,3,6,7-tetrahydroxyxanthone and -7.514 kcal/mol with acarbose. From an energy perspective, the binding affinity of 1,3,6,7-tetrahydroxyxanthone to α-glucosidase was weaker than the interaction between acarbose and α-glucosidase. A study conducted in 2022 revealed that the inhibitory activity of small-molecule ligands towards α-glucosidase is greatly influenced by hydrogen bonding and hydrophobic interactions (Sakulkeo et al., 2022).

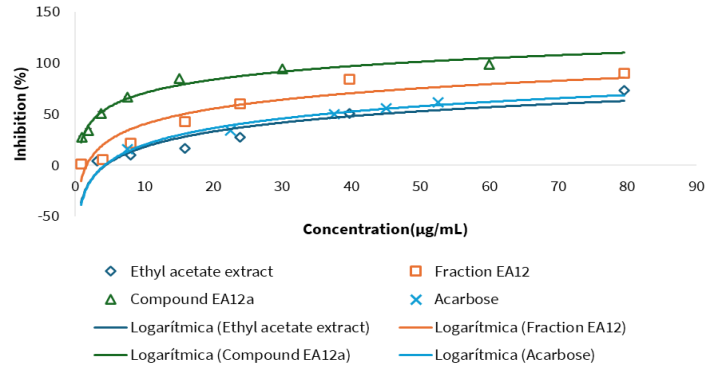


Figure 5. Inhibition of α-glucosidase enzyme by ethyl acetate extract, EA12 fraction, EA12a compound, and acarbose.

Data are expressed as the means of three independent determinations.

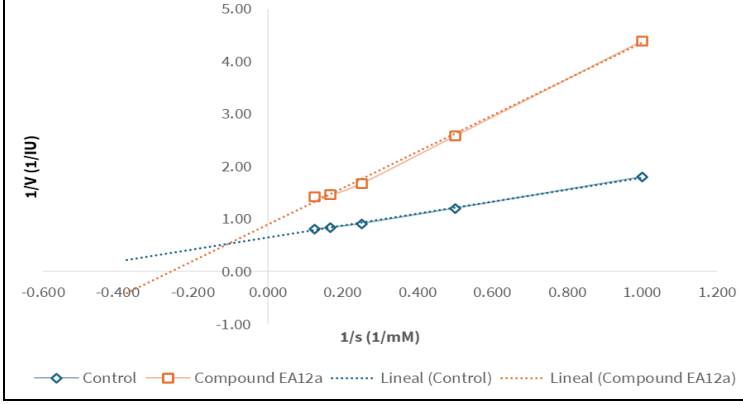


Figure 6. α-glucosidase kinetic analysis of compound EA12a.

Data are expressed as the means of three independent determinations.

Table 3. Binding energies of extracted compounds and acarbose with their corresponding hydrogen interacting residues.

Compound	Binding energy (kJ/mol)	Hydrogen bonding interacting residues and bond lengths (Å)
Acarbose	−7.514	Asp 404 (2.73, 2.57), His 674 (3.14), Asp 616 (2.59, 2.89), Arg 600 (2.87, 3.21), Asp 282 (2,64, 3.00), Met 519 (3,35)
1,3,6,7-tetrahydroxyxanthone	−7.087	Asp 518 (2.07), Asp 282 (2.95), Arg 600 (1.85)

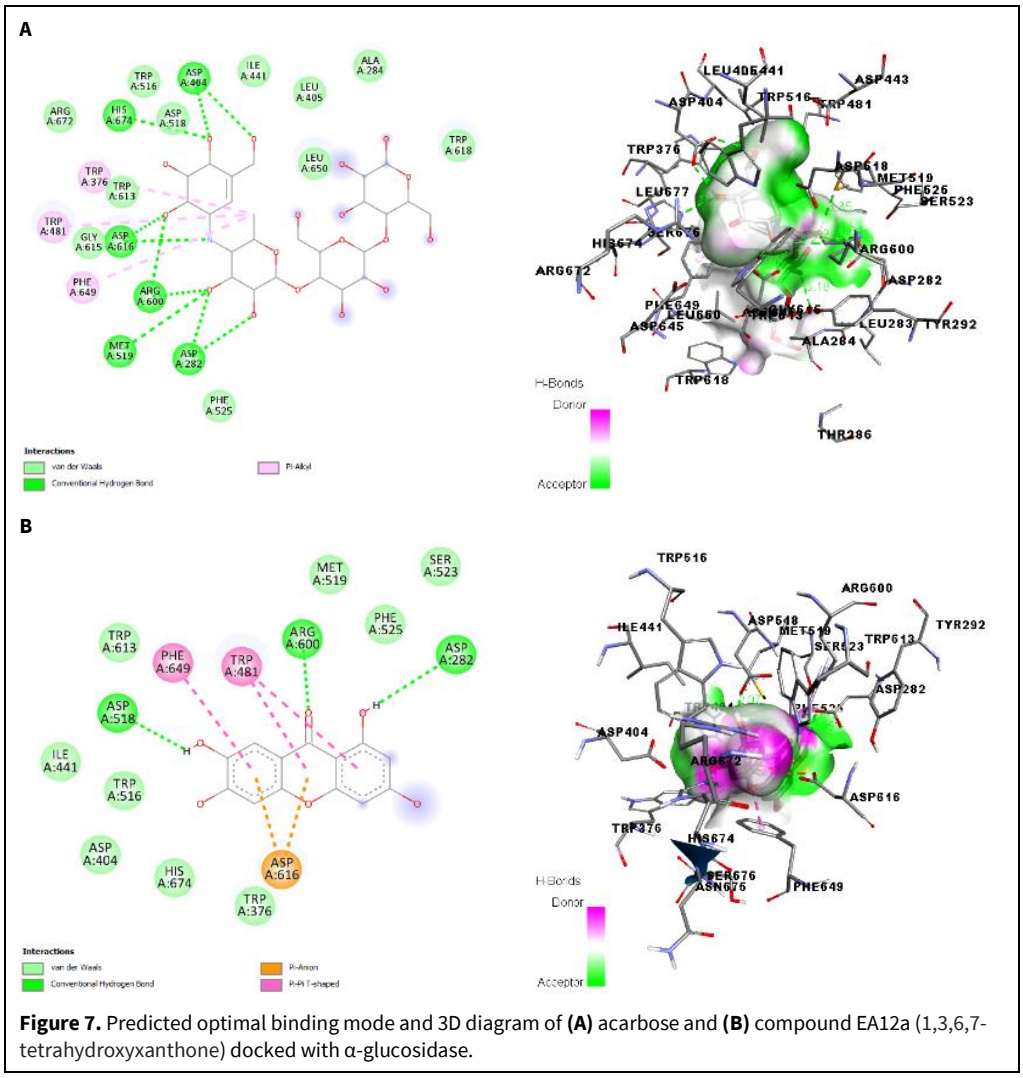


Figure 7. Predicted optimal binding mode and 3D diagram of **(A)** acarbose and **(B)** compound EA12a (1,3,6,7-tetrahydroxyxanthone) docked with α-glucosidase.

Table 3 shows that when acarbose was bound with α-glucosidase, six hydrogen bonds were formed between acarbose and the amino acid residues (Asp 404, His 674, Asp 616, Arg 600, Asp 282, and Met 519) (Fig. 7B). On the other hand, 1,3,6,7-tetrahydroxyxanthone formed three hydrogen bonds through its hydroxyl groups with Arg 600, Asp 518, and Asp 282 (Fig. 7A). In addition, another residue from the ligand, including Met 519, Ser 523, Ile 441, Phe 525, Trp 613, Trp 516, Trp 376, Asp 404, and His 674, can establish Van der Waals forces with the ligand. Out of three hydrogen bonds, the 1,3,6,7-tetrahydroxyxanthone only interacts with two similar residues if compared with the hydrogen bond in acarbose (Arg 600 and Asp 282). Furthermore, in addition to the variation in hydrogen bond count, the hydrogen bond formation sites between 1,3,6,7-tetrahydroxyxanthone or acarbose and amino acid residues contribute to differences in binding energy.

This implies that 1,3,6,7-tetrahydroxyxanthone's inhibitory effect does not rely on the number of hydrogen bonds or the similarity in amino acid binding site formation with acarbose. Therefore, further investigation is required to determine its precise inhibitory mechanism.

Physicochemical properties, pharmacokinetics, and toxicity prediction

In silico assessments of drug-likeness and ADMET characteristics can accurately forecast drug candidates' pharmacological and toxicological features in

the early phases of drug discovery, especially during the preclinical stage. *In silico* models have been utilized to enhance ADMET predictions.

Table 4 presents the drug-likeness values according to Lipinski's Rule of Five (Ro5) and Veber's rule. A molecule may be considered an effective drug candidate if it adheres to the permissible limits of physicochemical qualities as outlined by Lipinski's Rule of Five and Veber's criteria. Lipinski's Rule of Five was applicable if the compound's predictions met the established criteria, including a molecular weight of 500 Da or less, a maximum of 10 hydrogen bond acceptors (HBA), a maximum of five hydrogen bond donors (HBD), and a Consensus LogP for lipophilicity, alongside Veber's criteria, which define no more than 10 rotatable bonds and a topological polar surface area (TPSA) of 140 or less (Daina et al., 2017). Table 4 indicates that the compound EA12a exceeded the conventional thresholds of Lipinski's Rule of Five and Veber's Rule, suggesting it could attain favorable bioavailability upon oral administration. Nonetheless, acarbose failed to comply with Lipinski's Rule of Five and Veber's criteria. This may result in inadequate absorption into the systemic circulation from the small intestine. The outcome of this cannot be altered because the action site of the α-glucosidase inhibitor drugs is located in the small intestine, where it interacts with the α-glucosidase enzymes (Rosak and Mertes, 2012).

Table 4. Physicochemical properties, pharmacokinetics, drug-likeness, and toxicity of Compound EA12a and acarbose.

Property		Acarbose	Compound EA12A
Physicochemical properties	Molecular weight	645.60	260.20
	Hydrogen bond acceptors	19	6
	Hydrogen bond donor	14	4
	Rotatable bond	9	0
	Consensus LogP	-6.03	1.30
	TPSA	321.12	111.13
Pharmacokinetics	GI absorption	Low	High
	BBB permeant	No	No
	P-gp substrate	Yes	No
	CYP1A2 inhibitor	No	Yes
	CYP2C19 inhibitor	No	No
	CYP2C9 inhibitor	No	No
	CYP2D6 inhibitor	No	Yes
	CYP3A4 inhibitor	No	Yes
	Log K_p	-16.50	-6.40
Drug likeness	Lipinski	No, three violations	Yes, zero violation
	Veber	No, two violations	Yes
	Bioavailability	0.17	0.55
Toxicity	Hepatotoxicity	Active (0.50)	Inactive (0.73)
	Neurotoxicity	Inactive (0.57)	Inactive (0.90)
	Nephrotoxicity	Active (0.85)	Active (0.58)
	Respiratory toxicity	Active (0.68)	Active (0.78)
	Cardiotoxicity	Active (0.68)	Inactive (0.95)
	Carcinogenicity	Inactive (0.84)	Active (0.66)
	Immunotoxicity	Active (0.91)	Inactive (0.96)
	Mutagenicity	Inactive (0.76)	Active (0.58)
	Cytotoxicity	Inactive (0.69)	Inactive (0.96)

An ATP-binding cassette (ABC) transporter, exemplified by P-glycoprotein (P-gp), is a protein that plays a significant role in numerous essential activities, primarily in drug absorption, distribution, metabolism, and excretion (ADME) (Broccatelli et al., 2011). P-gp functions as a biological barrier by extruding xenobiotics and poisons from cells. In addition to the intestine, P-gp is expressed in several organs, including the liver, kidney, and the luminal membranes of the blood-brain barrier. It was predicted that compound EA12a was not a P-gp substrate, but acarbose would serve as a P-gp substrate. The interaction with P-gp substrates diminishes the overall absorption of these substances via the small intestine into the systemic circulation (Pires et al., 2015).

According to Table 4, compound EA12a was an inhibitor of cytochrome (CYP)3A4, CYP2D6, and CYP1A2 in metabolism properties. Therefore, caution is advised when used concomitantly with other drugs that are metabolized by the CYP3A4, CYP2D6, and CYP1A2 enzymes. In the toxicity prediction, compound EA12a was predicted to cause nephrotoxicity, respiratory toxicity, carcinogenicity, and mutagenicity. This is slightly different from acarbose, which is predicted to cause hepatotoxicity, nephrotoxicity, respiratory toxicity, cardiotoxicity, and immunotoxicity.

Antioxidant capacity

The DPPH radical scavenging method and FRAP assay measured the antioxidant activity. The free radical DPPH has become generally accepted as a test model for antioxidant activity due to its fast analytical approach, simplicity, sensitivity to samples even at low concentrations, and ease of use. The process in this test is based on reducing the unpaired electron on the nitrogen atom by the hydrogen atom of the antioxidant, which leads to the creation of a yellow hydrazine group. Any changes in the absorption of unreacted DPPH, compared to that of DPPH that has reacted with antioxidants, were measured using a spectrophotometer (Baliyan et al., 2022; El-Lateef et al., 2023; Phuyal et al., 2020).

Meanwhile, methods for FRAP assays utilize the fact that the antioxidant compounds act as electron donors, which enables the reduction process of the yellow Fe^{3+} complex molecule, potassium hexacyanoferrate, into a bluish-green Fe^{2+} complex compound through an acidic medium. Since a molecule's potential to be an antioxidant can be ascertained by its ability to reduce Fe^{3+} to Fe^{2+}, it is thus a measure of the reducing power. This is now possible because the antioxidant chemicals can either donate electrons or hydrogen atoms to stabilize the molecules that are still radicals (Benzie and Strain, 1996; Da Silva Borges et al., 2019; El-Lateef et al., 2023; Gligor et al., 2023).

A previous study by Mahayasih et al. (2018) tested the antioxidant capacity of an ethyl acetate extract of *G. lateriflora* leaves using scavenged radical DPPH and FRAP reagent, which showed EC_{50} values of 65.20 ± 0.45 µg/mL and 48.61 ± 0.32 µg/mL, respectively. The EC_{50} value of fraction EA12 and compound EA12a in this study can be shown in Table 2. Meanwhile, the comparison of the percent inhibition between ethyl acetate extract, fraction EA12, compound EA12a, and quercetin on scavenging the radical DPPH and reducing the FRAP reagent can be seen in Fig. 8A and 8B, respectively.

According to the data, compound EA12a possesses strong antioxidant activity in scavenging the radical DPPH and FRAP assay, with EC_{50} 21.31 ± 0.22 and 27.08 ± 0.26 µg/mL ($p<0.05$), respectively. Meanwhile, the EA12 fraction showed weak antioxidant activity. The different potency given by the sample is probably because of the effect of the fractionation and purification process. The compound in *G. lateriflora* leaves that has antioxidant capacity acted better as an antioxidant in the ethyl acetate extract than in the EA12 fraction. Even though the compound EA12a has a lower antioxidant capacity than the positive control, quercetin, it still has a strong antioxidant capacity and potential as an antioxidant agent.

The hydroxyl groups (OH) are primarily responsible for the high antioxidant capacity of phenolic compounds since they act as effective hydrogen donors. The planar molecular structure of phenolics can support conjugation and electron delocalization, which results in more stability for the formed radical. The general enhanced aromatic ring conjugation due to intramolecular hydrogen bonding between nearby hydroxyl and carbonyl groups increases hydrogen-donating ability based on radical delocalization. These two structural characteristics combined account for the potent antioxidant properties exhibited by compound 1,3,6,7-tetrahydroxyxanthone (Flieger et al., 2021; Gontijo et al., 2012).

A Pearson correlation analysis in Table 5 indicates that the relationship between α-glucosidase inhibitor and antioxidant capacity of ethyl acetate extract, fraction EA12, and compound EA12a from *G. lateriflora* was weak (FRAP) to moderate (DPPH) positive correlation, but not statistically significant ($p>0.01$). However, a statistically significant ($p<0.01$), very strong positive correlation was observed regarding the antioxidant capacity of DPPH and FRAP. The positive correlation indicated there is a linear correlation between the activity given.

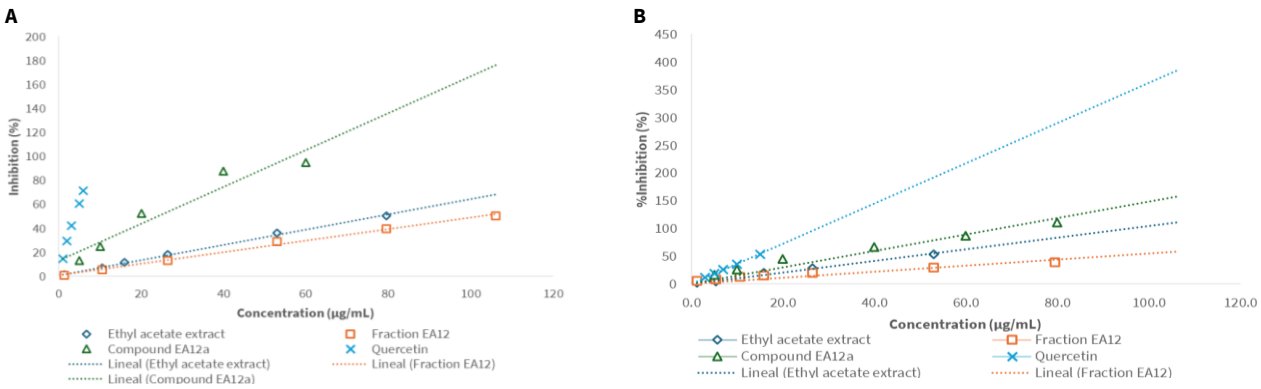


Figure 8. Comparison of the percent inhibition of the studied extract, fraction, compound EA12a, and quercetin on **(A)** scavenging the radical DPPH and **(B)** reducing the FRAP reagent.

Data are expressed as the means of three independent determinations.

Table 5. Pearson correlation of α-glucosidase inhibitor and antioxidant capacity (DPPH and FRAP) of ethyl acetate extract, fraction EA12, and compound EA12a.

Variable 1	Variable 2	Pearson correlation (r)	p-value	Interpretation
α-glucosidase inhibitor	DPPH	0.502	0.168	Moderate positive correlation, not significant
α-glucosidase inhibitor	FRAP	0.23	0.551	Weak positive correlation, not significant
DPPH	FRAP	0.951	0*	Very strong positive correlation, highly significant

*. Correlation is significant at the 0.01 level (2-tailed).

CONCLUSION

This study isolated a xanthone from an ethyl acetate extract of *G. lateriflora* leaves. Structure determination of the compound is done using LC-MS/MS and ^{1}H-NMR spectroscopic techniques, which was assumed to be 1,3,6,7-tetrahydroxyxanthone. In the light of in vitro and molecular docking studies, the compound EA12a has strong activity as an α-glucosidase inhibitor and may be considered an effective compound, 1,3,6,7-tetrahydroxyxanthone. Besides, it indicated a strong free radical scavenging property on DPPH and reducing FRAP assays.

CONFLICT OF INTEREST

The authors declare no conflicts of interest.

ACKNOWLEDGMENTS

This research did not receive any specific grant from funding agencies in the public, commercial, or not-for-profit sectors.

REFERENCES

Akmal M, Patel P, Wadhwa R (2024) Alpha Glucosidase Inhibitors. [Updated 2024 Feb 28]. In: StatPearls [Internet]. Treasure Island (FL): StatPearls Publishing; 2025 Jan-. https://www.ncbi.nlm.nih.gov/books/NBK557848/

Amelia P, Elya B, Hanafi M (2015) Antioxidative activity of xanthone from *Garcinia benthami* Pierre leaves. Int J PharmTech Res 7(2): 254-257.

Baliyan S, Mukherjee R, Priyadarshini A, Vibhuti A, Gupta A, Pandey RP, Chang CM (2022) Determination of antioxidants by DPPH radical scavenging activity and quantitative phytochemical analysis of *Ficus religiosa*. Molecules 27(4): 1326. https://doi.org/10.3390/molecules27041326

Benzie IF F, Strain JJ (1996) The ferric reducing ability of plasma (FRAP) as a measure of "antioxidant power": The FRAP assay. Anal Biochem 239(1): 70–76. https://doi.org/10.1006/abio.1996.0292

Broccatelli F, Carosati E, Neri A, Frosini M, Goracci L, Oprea TI, Cruciani G (2011) A novel approach for predicting P-glycoprotein (ABCB1) inhibition using molecular interaction fields. J Med Chem 54(6): 1740–1751. https://doi.org/10.1021/jm101421d

Da Silva Borges L, Pace Pereira Lima G, Artés F, De Souza ME, Freitas LS, De Jesus HI, Alves Santos NF, Da Silva Melo MR (2019) Efficiency of DPPH and FRAP assays for estimating antioxidant activity and separation of organic acids and phenolic compounds by liquid chromatography in fresh-cut nectarine. Aust J Crop Sci 13(7): 1053–1060. https://doi.org/10.21475/ajcs.19.13.07.p1368

Daina A, Michielin O, Zoete V (2017) SwissADME: A free web tool to evaluate pharmacokinetics, drug-likeness and medicinal chemistry friendliness of small molecules. Sci Rep 7(1): 42717. https://doi.org/10.1038/srep42717

Delita N, Elya B, Hanafi M (2020) Isolation and identification of chemical compounds from *Garcinia fruticosa* Lauterb stem bark extract. Pharmacogn J 12(6s): 1641–1652. https://doi.org/10.5530/pj.2020.12.224

Dirir AM, Daou M, Yousef AF, Yousef LF (2022) A review of alpha-glucosidase inhibitors from plants as potential candidates for

the treatment of type-2 diabetes. Phytochem Rev 21(4): 1049–1079. https://doi.org/10.1007/s11101-021-09773-1

El-Lateef HMA, El-Dabea T, Khalaf MM, Abu-Dief AM (2023) Recent overview of potent antioxidant activity of coordination compounds. Antioxidants 12(2): 213. https://doi.org/10.3390/antiox12020213

Elwekeel A, Amir D El, Mohamed EIA, Amin E, Zaki MA (2022) Characterization of possible α-glucosidase inhibitors from *Trigonella stellata* extract using LC–MS and *in silico* molecular docking. Plants 11(2): 208. https://doi.org/10.3390/plants11020208

Espirito Santo BLSD, Santana LF, Kato Junior WH, de Araújo FO, Bogo D, Freitas KC, Guimarães RCA, Hiane PA, Pott A, Filiú WFO, Arakaki Asato M, Figueiredo PO, Bastos PRHO (2020) Medicinal potential of *Garcinia* species and their compounds. Molecules 25(19): 4513. https://doi.org/10.3390/molecules25194513

Flieger J, Flieger W, Baj J, Maciejewski R (2021) Antioxidants: Classification, natural sources, activity/capacity measurements, and usefulness for the synthesis of nanoparticles. Materials 14(15): 4135. https://doi.org/10.3390/ma14154135

Gligor O, Clichici S, Moldovan R, Muntean D, Vlase AM, Nadăş GC, Matei IA, Filip GA, Vlase L, Crişan G (2023) The effect of extraction methods on phytochemicals and biological activities of green coffee beans extracts. Plants 12(4): 712. https://doi.org/10.3390/plants12040712

Gontijo VS, De Souza TC, Rosa IA, Soares MG, Da Silva MA, Vilegas W, Viegas C, Dos Santos, MH (2012) Isolation and evaluation of the antioxidant activity of phenolic constituents of the *Garcinia brasiliensis* epicarp. Food Chem 132(3): 1230–1235. https://doi.org/10.1016/j.foodchem.2011.10.110

Huang Q, Wang Y, Wu H, Yuan M, Zheng C, Xu H (2021). Xanthone glucosides: Isolation, bioactivity and synthesis. Molecules 26(18): 5575. https://doi.org/10.3390/molecules26185575

Mahayasih PGMW, Elya B, Hanafi M (2017) Alpha-glucosidase inhibitory activity of *Garcinia lateriflora* Blume leaves. J App Pharm Sci 7(10): 100–104. https://doi.org/10.7324/JAPS.2017.71014

Mahayasih PGMW, Elya B, Hanafi M (2018) Fractionation and antioxidant activity potency of the extract of *Garcinia lateriflora* Blume var. javanica Boerl leaf. AIP Conf Proc 1933: 030018. https://doi.org/10.1063/1.5023965

Mottaghipisheh J, Kamali M, Doustimotlagh AH, Nowroozzadeh MH, Rasekh F, Hashempur MH, Iraji A (2024) A comprehensive review of ethnomedicinal approaches, phytochemical analysis, and pharmacological potential of *Vitex trifolia*. Front Pharmacol 15: 1322083. https://doi.org/10.3389/fphar.2024.1322083

Nur S, Hanafi M, Setiawan H, Nursamsiar, Elya B (2023) *In silico* evaluation of the dermal antiaging activity of *Molineria latifolia* (Dryand. ex W.T. Aiton) Herb. Ex Kurz compounds. J Pharm Pharmacogn Res 11(2): 325–345. https://doi.org/10.56499/jppres23.1606_11.2.325

Ogurtsova K, da Rocha Fernandes JD, Huang Y, Linnenkamp U, Guariguata L, Cho NH, Cavan D, Shaw JE, Makaroff LE (2017) IDF Diabetes Atlas: Global estimates for the prevalence of diabetes for 2015 and 2040. Diabetes Res Clin Pract 128: 40–50. https://doi.org/10.1016/j.diabres.2017.03.024

Pires DEV, Blundell TL, Ascher DB (2015) pkCSM: Predicting small-molecule pharmacokinetic and toxicity properties using graph-based signatures. J Med Chem 58(9): 4066–4072. https://doi.org/10.1021/acs.jmedchem.5b00104

Phuyal N, Jha PK, Raturi PP, Rajbhandary S (2020) Total phenolic, flavonoid contents, and antioxidant activities of fruit, seed, and bark extracts of *Zanthoxylum armatum* DC. Sci World J 2020: 8780704. https://doi.org/10.1155/2020/8780704

Rosak C, Mertes G (2012) Critical evaluation of the role of acarbose in the treatment of diabetes: Patient considerations. Diabetes Metab Syndr Obes 5: 357-367. https://doi.org/10.2147/DMSO.S28340

Rouzbehan S, Moein S, Homaei A, Moein MR (2017) Kinetics of α-glucosidase inhibition by different fractions of three species of *Labiatae* extracts: A new diabetes treatment model. Pharm Biol 55(1): 1483–1488. https://doi.org/10.1080/13880209.2017.1306569

Sakulkeo O, Wattanapiromsakul C, Pitakbut T, Dej-Adisai S (2022) Alpha-glucosidase inhibition and molecular docking of isolated compounds from traditional Thai medicinal plant, *Neuropeltis racemosa* Wall. Molecules 27(3): 639. https://doi.org/10.3390/molecules27030639

Shen H, Wang J, Ao J, Cai Y, Xi M, Hou Y, Li M, Luo A (2022) Inhibitory kinetics and mechanism of active compounds in green walnut husk against α-glucosidase: Spectroscopy and molecular docking analyses. LWT 172: 114179. https://doi.org/10.1016/J.LWT.2022.114179

Subhan M, Sanachai K, Sungthong B, Datham S, Ratha J, Puthongking P (2025) Comparison *in vitro* and *in silico* studies of phenolic acids and flavonoids on α-glucosidase inhibition. J Pharm Pharmacogn Res 13(1): 311–323. https://doi.org/10.56499/jppres24.2081_13.1.311

AUTHOR CONTRIBUTION:

Contribution	Mahayasih PGMW	Hanafi M	Eden Y	Maulana D	Triadisti N	Elya B
Concepts or ideas	x	x	x			x
Design	x	x	x			x
Definition of intellectual content	x	x	x	x	x	x
Literature search	x	x	x	x		x
Experimental studies	x	x	x	x	x	x
Data acquisition	x	x	x	x	x	x
Data analysis	x	x	x	x	x	x
Statistical analysis	x	x	x	x		x
Manuscript preparation	x			x		x
Manuscript editing	x					x
Manuscript review	x	x	x	x	x	x

Citation Format: Mahayasih PGMW, Hanafi M, Eden Y, Maulana D, Triadisti N, Elya B (2025) A xanthone from *Garcinia lateriflora* Blume leaves extract: Isolation, α-glucosidase inhibitory activity, and antioxidant capacity. J Pharm Pharmacogn Res 13(4): 1275–1287. https://doi.org/10.56499/jppres24.2178_13.4.1275

Publisher's Note: All claims expressed in this article are solely those of the authors and do not necessarily represent those of their affiliated organizations, or those of the publisher, the editors and the reviewers. Any product that may be evaluated in this article, or claim that may be made by its manufacturer, is not guaranteed or endorsed by the publisher.

Open Access: This article is distributed under the terms of the Creative Commons Attribution 4.0 International License (http://creativecommons.org/ licenses/by/4.0/), which permits use, duplication, adaptation, distribution and reproduction in any medium or format, as long as you give appropriate credit to the original author(s) and the source, provide a link to the Creative Commons license and indicate if changes were made.